Dynamic Behavior and Substrate Interactions of the Polymyxin Resistance Determinant MCR-1 Investigated by Extended Molecular Dynamics Simulations in the Membrane Environment

Emily Lythell,[a,b] Reynier Suardíaz,[a,c#,d] Philip Hinchliffe[b], A Sofia F Oliveira[a], Marc W. Van der Kamp[d], James Spencer,[b]* Adrian J. Mulholland[a]*

a. Centre for Computational Chemistry, School of Chemistry, University of Bristol, Cantock's Close, Bristol BS8 1TS, UK.

b. School of Cellular and Molecular Medicine, University of Bristol, University Walk, Bristol BS8 1TD, UK.

c. Departamento de Química Física, Facultad de Química, Universidad Complutense, 28040 Madrid, Spain.

d. School of Biochemistry, University of Bristol, University Walk, Bristol BS8 1TD, UK.

[#]present address

*corresponding authors Jim.Spencer@bristol.ac.uk; Adrian.Mulholland@bristol.ac.uk

Keywords: antimicrobial resistance, molecular dynamics, polymyxin, MCR-1, phosphoethanolamine transferase

Abstract

The polymyxin colistin is an agent of last resort for treatment of severe infections by multiresistant Gram-negative opportunistic bacteria. Colistin resistance arises through covalent modification of lipid A disaccharide by phosphoethanolamine (PEtN) transferases, preventing colistin interaction. The Mobile Colistin Resistance (MCR) PEtN transferase is a plasmid-borne enzyme that is the major cause of colistin resistance in *Escherichia coli*, the most important antimicrobial resistant bacterial pathogen worldwide. Bacterial PEtN transferases like MCR comprise periplasmic catalytic and integral membrane domains, with mechanistic understanding largely based on studies of the former with limited information on the full-length enzyme. Previous investigations of a *Neisseria meningitidis* PEtN transferase identified that the catalytic domain can effectively dissociate from the transmembrane component and instead make extensive contacts with the membrane surface. Here we report extended molecular dynamics simulations of a model of full-length MCR-1, in a representative membrane comprising 80% of a PEtN donor substrate palmitoyloleoyl phosphoethanolamine (POPE) that explore the dynamic behavior of the enzyme and the impact upon it of zinc stoichiometry and of PEtN addition to the Thr285 acceptor residue. The results identify only limited movement of the two domains relative to one another, and that POPE can bind the likely “resting” state of the enzyme (mono-zinc with unmodified Thr285) in an orientation compatible with PEtN transfer to Thr285. Our data suggest domain motions in bacterial PEtN transferases to be condition-dependent and support a proposed “ping - pong” reaction mechanism with the mono-zinc enzyme competent to undertake the first stage.

Introduction

Bacterial antimicrobial resistance (AMR) is a key global public health challenge. Estimates based on 2019 data[1] identify 1.3m deaths worldwide as directly attributable to AMR, with AMR a contributing factor to a further 3.7m. A previous study[2] projected an annual total of 10m deaths by 2050 in the absence of effective interventions. Two species of Enterobacterales, *Escherichia coli* and *Klebsiella pneumoniae*, are respectively the first and third most common pathogens responsible for AMR-associated deaths. Strains of these organisms resistant to carbapenems or extended-spectrum oxyimino cephalosporins are considered by the World Health Organization to be critical priority pathogens for antimicrobial research and development[3] due to the weakness of the antibacterial discovery pipeline for these and other multiresistant Gram-negative bacteria.

Polymyxin antibiotics, specifically colistin, are agents of last resort for treating infections by these species[4] and, despite toxicity concerns[5], their use has increased in recent years[6]. Polymyxins disrupt the Gram-negative envelope by a sequential process that remains incompletely understood[7]: initial interaction with outer membrane lipopolysaccharide (LPS) is followed by uptake into the bacterial periplasm and effects upon the inner membrane that may include interference with LPS before or during trafficking to the outer membrane and/or direct permeabilization. In consequence, modifications to LPS that disrupt polymyxin interactions are determinants of polymyxin resistance; specifically, these reduce negative charges on the lipid A disaccharide by covalent modification of phosphate groups, thereby preventing electrostatic interactions with cationic components of the polymyxin peptide. Such modifications most commonly involve addition of phosphoethanolamine (PEtN) (**Scheme 1A**) or 4-amino-4-deoxy-L-arabinose (L-Ara-4N) to the 1' or 4' phosphates[8].

Lipid A phosphoethanolamine transferases are widely distributed in Gram-negative bacteria, and are constitutively expressed in some species, including *Neisseria meningitidis*[9] and *Moraxella catarrhalis*[10], that in consequence are intrinsically polymyxin-resistant. In others, including *Acinetobacter baumannii*[11], acquired polymyxin resistance can arise from upregulation of chromosomal PEtN transferases, but in *E. coli* this has remained rare. In 2015 however, a plasmid-borne polymyxin resistance determinant, the Mobile Colistin Resistance (MCR)-1 PEtN transferase, was identified in China in an *E. coli* isolate of porcine origin[12], since when multiple MCR isoforms have been discovered in multiple species worldwide[13]. In *E. coli* MCR production remains the dominant polymyxin resistance mechanism.

Phosphoethanolamine transferases, including MCR, are enzymes of the Gram-negative inner membrane that consist a soluble periplasmic catalytic and a transmembrane domain[14] (**Figure 1**). The catalytic domain has been the subject of relatively extensive biochemical study[15-17] and contains a zinc site (Zn1, comprised of three conserved amino acids, Glu246, Asp 465 and His466) adjacent to the threonine residue (Thr285) that is the likely site of formation of the covalent phosphointermediate formed when PEtN is transferred from a phosphatidyl ethanolamine donor to the lipid A acceptor substrate (**Scheme 1**). Two additional conserved "gating" histidine residues (His395 and His478) are observed in some structures[15] to bind a second zinc equivalent (Zn2), but the physiological and mechanistic significance of this site remains unclear. The contribution of the transmembrane domain to MCR activity is also incompletely understood, although it is reasonable to assume involvement in binding both (lipdated) donor and acceptor substrates, and potentially in orienting these for PEtN transfer. Given that the majority of studies have investigated the isolated MCR catalytic domain, it is also an open question as to whether residues from the transmembrane domain, in particular Glu116 positioned on a short α-helix that sits on the inner membrane surface, form part of the active site in the intact protein and hence are important in catalyzing the PEtN transfer reaction.

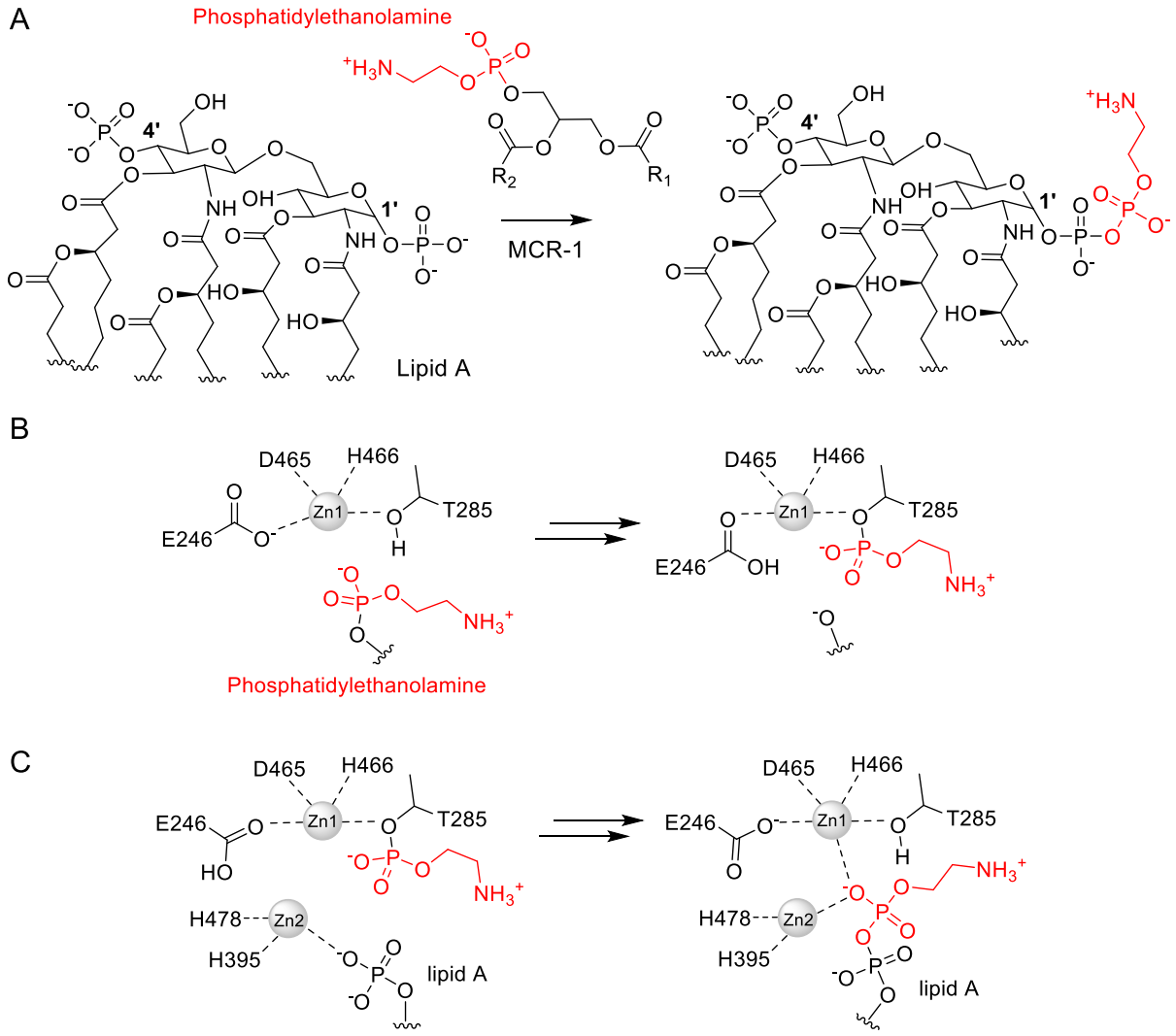

Scheme 1. Phosphoethanolamine Transfer to Lipid A Catalyzed by MCR-1. (A) Overall reaction involves transfer of phosphoethanolamine to the 1' or 4' phosphate group of lipid A. This likely occurs via a ping-pong mechanism, involving two distinct steps: **(B)** First step of the proposed ping-pong reaction in a mono-zinc active site involves transfer of phosphoethanolamine (red, from a phosphatidylethanolamine donor) to Thr285. **(C)** Second step (proposed to require a dizinc active site) involves transfer of phosphoethanolamine to lipid A, and reprotonation of Thr285. Adapted from Suardíaz *et al*[18].

To date, an experimentally determined structure is only available for one PEtN transferase, the chromosomally encoded EptA enzyme from *N. meningitidis*[14]. On the basis of this structure, these authors undertook a series of molecular dynamics (MD) simulations of EptA within the membrane environment, and in two of six 100 ns trajectories observed the enzyme to undergo a significant conformational change in which the catalytic domain underwent a rotation about the loop connecting the two domains, relative to the transmembrane domain and the membrane, allowing for new membrane contacts and even deformation of the membrane surface. It was hypothesized that this flexibility could allow for entry to the active site of two substrates of differing sizes, and so may be important to reactivity of the enzyme. Biophysical studies[19], primarily using small-angle X-ray scattering (SAXS), were considered to support this contention by identifying differences in the

conformation of *N. meningtidis* EptA in micelles of two different detergents, *n*-dodecyl-β-d-maltoside (DDM) and *n*-dodecyl-phosphocholine (DPC), with the latter promoting a more open, extended organization. To date, however, no such investigations have been reported for any MCR enzyme.

Accordingly, and building on our previous computational investigations of the isolated MCR catalytic domain, we here sought to explore the conformational dynamics of the complete MCR protein using extended (500 ns) molecular dynamics simulations of an homology model in a model membrane environment, in order to investigate interactions with the phosphatidylethanolamine donor substrate and zinc cofactor in the ground (reactive) state, and the effect upon these of PEtN addition to Thr285 to form the covalent phosphointermediate. The results identify only limited motions of the two domains relative to one another and do not support stable binding of a second zinc equivalent under the conditions tested, while establishing that the complex of a donor substrate with the ground state enzyme is capable of sampling a stable and potentially reactive conformation.

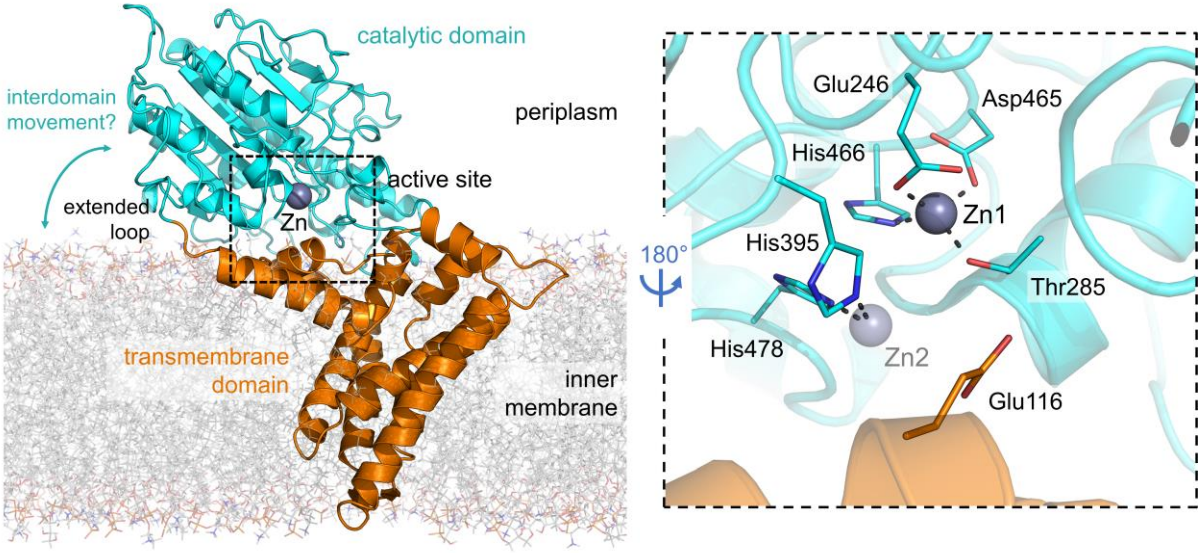

Figure 1. Architecture of MCR-1. *Left,* overall architecture of MCR-1 (homology model derived from the full-length structure of EptA, PDB 5FGN[14]). *Boxed*, active site of MCR-1 based on the crystal structure of the dizinc form of the catalytic domain (PDB 5LRM[15]). Hydrogen and co-ordination bonds are shown as dashed lines.

Materials and Methods

Model construction

An homology model of full-length MCR-1 (Figure S1) was created using Modeller v. 9.17[20], using the *N. meningitidis* EptA[14] structure (PDB 5FGN, 35.6 % sequence identity) as a template. To create a di-zinc starting structure, the second zinc equivalent was positioned by aligning this model with the structure of the MCR-1 catalytic domain in the di-zinc form (PDB 5LRM[15]). The final model comprises MCR-1 residues 11 - 541; the first ten residues were excluded as these form an unstructured N-terminal tail far from the active site and have no predicted structural or catalytic function. Phosphorylated Thr285, as found in the structure of MCR-1 in the mono-zinc form (PDBPDB 5LRN[15]), was modified to threonine and to phosphoethanolaminated threonine (PET) using the builder tool in PyMOL[21], to replicate the resting and phosphointermediate states, respectively. The sidechain of the phosphoethanolaminated threonine (PET) residue was positioned to avoid sidechain clashes with residues from either domain. The engineered PET residue was parameterized using the RED server with QM optimization using Gaussian[22].

MD Simulations

The CHARMM-GUI web server was then used to create hydrated, membrane-bound MCR-1 systems for MD simulations[23]. The protein was oriented in the membrane using the PPM server[24] option on the protein chain. A heterogeneous lipid bilayer was built in a rectangular box with the Z dimension determined by the thickness of the water shell (20 Å) and the X and Y dimensions by the numbers of lipid components, keeping the two values equal to one another. The bilayer was composed of a mixture of palmitoyloleoyl phosphoethanolamine (POPE) and palmitoyloleoyl phosphatidylglycerol (POPG) lipids in an approximate 80:20 ratio. The upper leaflet was comprised of 302 POPE and 75 POPG lipids, and the lower leaflet of 320 POPE and 80 POPG lipids, to account for the reduced intracellular cross-sectional area of the protein relative to the extracellular area. This produced a final system size of *c*. 156 x 156 x 124 Å. The membrane was built using a replacement method, which involved one POPE residue being modelled into the active site. $CaCl_2$ ions were included using a distance ion placing method[25] to neutralize the system, with a final concentration of 0.1 M. Input files were generated by the web server for AMBER using NPT ensemble at 300 K, using ff14SB[26] for protein, lipid17[27] for lipids, and TIP3P for water[28] after membrane building[25, 29]. The bound zinc ion(s) were parameterised using the standard 12-6 Lennard-Jones (LJ) nonbonded model[30]. During the membrane building step, a POPE phospholipid was modelled into the active site; this was deleted from the system in models without bound phospholipid. The various systems were minimized using the AMBER engine pmemd.MPI for 500 steps using a non-bonded cut-off of 9.0 Å, with harmonic positional restraints on the protein (weight 10.0), and on the membrane (weight 2.5). NPT equilibration was performed at 300 K (except where stated) using the Berendsen barostat and Langevin dynamics with $\gamma = 1.0\ ps^{-1}$, a non-bonded cut-off of 9.0 Å, and applying SHAKE[31] restraints. The equilibration was performed over six steps with parameters specified in **Table S1**. For each system tested three production runs, each of 500 ns, were then carried out.

Where employed, coordination of the Zn1 (by Glu246 OE2, Thr285 OD1, Asp465 OD1 and His466 NE2) and Zn2 (by His395 NE2 and His478 NE2) zinc ions was restrained to the distances observed in the crystal structure 5LRM[15], and the pairwise angles between them (set to reference value ± 10.0°) with restraint values of 25 kcal $mol^{-1}Å^2$.

Results

Dynamic Behavior of Full-Length MCR-1

In previous work[15, 18, 32] we applied structural, microbiological and computational methods to investigate the mechanism of the MCR-1 phosphoethanolamine transferase, focusing on the isolated periplasmic catalytic domain as a tractable model system. Here we extend these studies to address the behavior of the intact (full-length) enzyme, including both the catalytic and N-terminal transmembrane (TMD) domains, in a representative *E. coli* inner membrane system; focusing on the interactions between the two domains and of the full-length protein with the zinc cofactor and palmitoyloleoyl phosphoethanolamine (POPE) donor substrate. In the absence of an experimental structure of full-length MCR-1, these investigations utilized an homology model (**Figure S1**) constructed based on our experimental structure of the MCR-1 catalytic domain (PDB 5LRN[15]) and on the crystal structure of the homologous *Neisseria meningitidis* EptA enzyme (PDB 5FGN[14]). The model comprises MCR-1 residues 11 - 541; with the first ten residues, that form an unstructured N-terminal tail, being excluded due to the absence of any predicted secondary structure, structural or catalytic function; as well as their situation far from the active site. The model was then tested in extended (triplicate 500 ns) molecular dynamics (MD) simulations in a rectangular model membrane system comprising a mixture of POPE and palmitoyloleoyl phosphatidylglycerol (POPG) in an 80:20 ratio. Eight sets of simulations tested MCR-1 in the mono- and dizinc forms, each in the presence and absence of a molecule of POPE docked into the active site cavity and with and without covalent attachment of phosphoethanolamine (PEtN) to the catalytic threonine residue Thr285. Simulations involving the PEtN-bound forms then represent possible states of the intermediate, expected to be formed after transfer of PEtN from a POPE donor to MCR-1, prior to reaction with the lipid A PEtN acceptor.

MD simulations of all eight systems converged after approximately 50 ns of simulation time, in each case to structures that remained close (≤ 4.0 Å) to the starting model, as evidenced by plots of Cα RMSD values averaged across the latter part (50 – 500 ns) of the simulations (**Figure S2**). Comparisons of Cα RMSD values for the two individual domains identified that the major contribution to these values arises from the changes in the transmembrane domain rather than the catalytic domain. Consistent with our previous finding that the isolated catalytic domain behaves as a rigid, stable entity, comparison of catalytic domain structures in frames extracted from simulations of the truncated and full-length proteins (**Figure S3**) identifies only minor differences localized to three regions: residues 219 – 234 that form the N-terminus of the isolated catalytic domain; residues 414 – 424 that form a surface loop that is undefined in some crystal structures (e.g. 5LRM[15]) and sits close to the membrane surface; and residues 298 – 305 that are also positioned to contact the membrane. An overall Cα RMSD of 1.79 Å, however, supports our previous conclusion that the secondary and tertiary structure of the periplasmic MCR-1 catalytic domain is largely unaffected by the presence of the transmembrane domain and/or the membrane itself.

It is also evident that the presence of the POPE donor substrate does not exert any significant effect upon the overall structure of either domain. The largest differences between equivalent sets of simulations in the absence and presence of POPE are observed for the "resting" (i.e. with Thr285 unmodified) state of the catalytic domain, and for the transmembrane domain in the PEtN-bound intermediate state, both in the mono-zinc form. In both cases we consider these differences to arise from stochastic variations between individual simulations in each set of triplicate repeats. For the unmodified mono-zinc system this variation is due to a reorientation of the two domains relative to one another in one of the three POPE-bound simulations, while in the intermediate (PEtN-bound) system the major differences involve unstructured loop regions, far from the active site, in both

catalytic and transmembrane domains. Less pronounced (≤ 4.0 Å) differences are also evident in all four helices of the transmembrane domain which interact with the POPE molecule (below). Overall, we conclude that increases in fluctuations within the MCR-1 structure in the presence or absence of docked POPE are due to stochastic variations between repeat simulations, and/or minor rearrangements within the transmembrane domain local to the POPE molecule, and do not indicate long-distance or larger scale conformational changes.

Domain Orientations During Simulations of Membrane-Bound MCR-1

These analyses indicate that the complete MCR-1 bound system retains a conformation close to that of the starting structure throughout the duration of the simulations; i.e. that both the structures of the individual domains, and their orientations relative to one another, are largely preserved during 500 ns of MD simulations in this model membrane environment. To further verify the latter conclusion, the distances between the respective centers of mass of the catalytic domain (residues 219 - 541) and transmembrane domain (residues 11 - 218) were plotted over time (50 – 500 ns) as averages ± 2 standard deviations (**Figure 2B**). Consistent with analysis of Cα RMSD values, the interdomain distance remains within a constant range throughout the simulations, providing no evidence that, over a time scale of 500 ns, changes in zinc stoichiometry, PEtN addition to Thr285, or presence/absence of the POPE donor substrate result in global changes to MCR-1 conformation. Specifically, none of our simulations identify the substantial changes in interdomain distance that would be expected were MCR-1 to be undergoing conformational transitions involving large-scale motions of the catalytic relative to the transmembrane domain, as previously observed in EptA[14]. As shown in **Figure 2A**, while some variation in domain positions in the individual simulations is evident, reflecting both repositioning of the transmembrane domain within the membrane and some limited reorientation of the two domains relative to one another, we do not observe the loss of interdomain interactions, and close association of the periplasmic domain with the membrane surface, described by Anandan *et al* in their studies of *N. meningitidis* EptA[14, 19].

In that work, such motions were observed in simulations at both 298 and 310 K. Accordingly, to investigate whether MCR-1 might experience increased mobility in simulations at physiological (i.e. host) temperature, a further set of triplicate 500 ns simulations of MCR-1 in the mono-zinc form, without bound POPE, was undertaken. The results failed to identify any significant change in dynamic behavior in simulations at the two different temperatures, as evidenced by averaged Cα RMSDs for simulations of the complete protein (2.70 ± 0.29 Å, 3.43 ± 0.48 Å); catalytic (1.55 ± 0.17 Å, 1.60 ± 0.16 Å) and transmembrane domains (2.73 ± 0.35 Å, 3.08 ± 0.48 Å) at 300 K and 310 K, respectively. Similarly, no significant difference was evident in the interdomain distance (39.4 ± 0.87 Å at 300 K, and 40.1 ± 0.57 Å at 310 K).

Interactions of Full-Length MCR-1 with Zinc Ions

Multiple crystal structures have been determined for the isolated soluble periplasmic catalytic domain of MCR-1[15, 16, 33]. These include a range of metalation states (i.e. zinc equivalents) and with the PEtN acceptor residue Thr285 in unmodified and phosphorylated forms. On the basis of these structures we have used MD simulations and QM cluster model calculations[18, 32] to propose that, in the isolated catalytic domain, the Zn1 ion is stably coordinated while the Zn2 site can retain its metal ion only in the presence of the lipid A acceptor, i.e. during the final step of the PEtN transfer reaction from Thr285 to the lipid A phosphate. However, such simulations necessarily neglect the possible involvement of

residues from the transmembrane domain in zinc coordination. Accordingly, we used our MD simulations to study the stability and coordination of both zinc ions in full-length MCR-1, in the absence and presence of PEtN bound to Thr285.

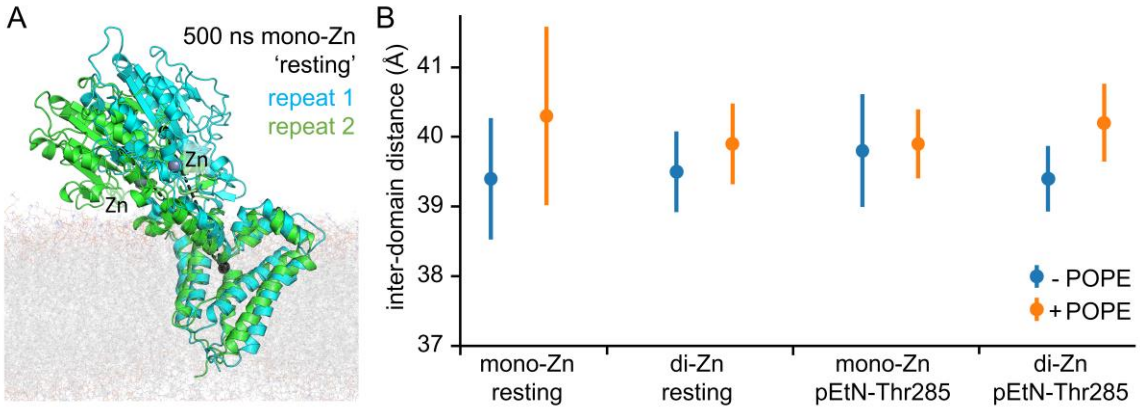

Figure 2. Movement of the Catalytic Domain Relative to the Transmembrane Domain in MD Simulations of Membrane-Bound MCR-1. A. Comparison of domain orientations in the final frames of two 500 ns MD simulations (repeat 1, cyan; repeat 2, green) of monozinc MCR-1 with a POPE molecule docked in the lower active site cleft. Repeat 2 closely matches the starting structure (C_α RMSD 2.98 Å ±0.15). Centers of mass (used for calculations in panel (b)) for the transmembrane (residues 11-218) and catalytic (residues 219 – 541) domains are shown as black spheres; dashed lines show the distance between the two. Zinc ions are shown as gray spheres. B. average interdomain distances during MD simulations. Distances between domain centers of mass in each of the eight sets of simulations are calculated as the means of all distances (one measurement per ns between 50 - 500 ns of each simulation) for the three replicate simulations of each system, plotted as circles ± 2 SD.

As in our previous studies of the isolated catalytic domain[32], in mono-zinc MCR-1 the zinc ion remains stably bound in the Zn1 site for the full 500 ns of our simulations. As before, in these simulations Zn1 favored 6 co-ordinate geometry as a consequence of our use of the Lennard-Jones 12-6 parameters to treat the metal ions, with this change in coordination achievable through a move to bidentate coordination by the two carboxylate ligands Glu246 and Asp465. The main change in active site geometry observed in these simulations is a reorientation of the transmembrane domain residue Glu116 in 2 out of 3 replicate simulations, that facilitates H-bonding to the side chain of His395 (**Figure S4A**). Similarly, when Thr285 is modified by addition of PEtN, while Zn1 coordination now involves one of the phosphoryl oxygen atoms in place of the Thr hydroxyl group, the metal center is otherwise stable, with reorganization of the system over the time scale of the simulation involving the PEtN moiety sampling alternative orientations through fluctuating H-bonds to His395, His478 and Glu116 (**Figure S4B**).

In simulations of the isolated MCR-1 catalytic domain in the di-zinc form, the Zn2 site, formed in crystal structures by His395 and His478, is unstable with bound zinc generally dissociating from unmodified (i.e. with free Thr285) enzyme over the course of 300 ns MD simulations[32]. In contrast, in equivalent simulations with full-length MCR-1, a second zinc ion is retained over the complete duration of all three 500 ns simulations reported here. However, across the three replicate simulations Glu116 from the transmembrane domain is the only protein ligand that retains interaction with the second zinc equivalent, with interactions with the "gating" histidine residues, in particular His395, being lost in two of the three repeats. This behavior is replicated when Thr285 is modified through addition of

PEtN; i.e. from a starting point close to the position of the Zn2 ion in the crystal structure of the di-zinc catalytic domain (PDB 5LRM[15]) the second zinc equivalent migrates away from the MCR-1 active center towards the solvent-exposed periphery of the protein, but is prevented from dissociating altogether by persistent contact with Glu116. Thus, despite the potential for residues from the transmembrane domain of MCR-1, in particular Glu116, to contribute to a more stable, physiological Zn2 site, our simulations do not support existence of stable di-zinc forms of MCR-1 in either the "resting" ground state or after modification of Thr285 through addition of PEtN.

Interactions of Full-Length MCR-1 with the POPE Donor Substrate

As detailed above, interactions of the PEtN donor substrate POPE were investigated with the various forms of MCR-1. As a starting point for these simulations, POPE was modelled into the MCR-1 active site, with the position of one of the two acyl tails based upon the position of the acyl chain of the dodecyl-beta-d-maltoside (DDM) detergent molecule in the *N. meningitidis* EptA structure[14].

In the various simulations of POPE-bound MCR-1, one of the two POPE acyl tails spends most of the simulation duration packed against helix α3 of the transmembrane domain (**Figure 3A**, residues Tyr74 - Thr94), with frequent additional interactions with helix α4 (Ala123 - Val143). Interactions with the MCR-1 active site are however more variable. In the "resting" (mono-zinc) state, where Thr285 is unmodified by PEtN, the POPE PEtN head group interacts with the conserved "gating" histidine residues His395 and (less commonly) His478, that bind the second zinc equivalent (Zn2) in crystal structures of the MCR-1 catalytic domain in the di-zinc form. These interactions are mediated by the terminal primary amine of the PEtN head group. The PEtN phosphate group can then variably contact any of three charged residues, Glu116, Asn108, and Tyr97, on the periplasmic face of the transmembrane domain. In one of the three replicate simulations, however, the POPE head group reorients to a position where it more deeply penetrates the catalytic domain, with the phosphate group approaching the terminal hydroxyl of the PEtN acceptor Thr285. After 500 ns this simulation has reached an equilibrium state (**Figure 3B**) with many features of a potentially reactive conformation, with a distance of 3.7 Å between the nucleophile (Thr285 Oγ) and electrophile (POPE phosphorous) of the first (PEtN transfer) step of the lipid A modification reaction.

Addition of PEtN to Thr285 however prevents POPE from accessing the active site. There is persistent interaction between the phosphate group of Thr285-bound PEtN and the active site zinc ion, replicating interactions observed in crystal structures (e.g. PDBPDB 5LRN[15]) that contain phosphorylated Thr285, and in the simulations described above. The ethanolamine moiety can then make more transient contacts with the "gating" residues His395 and/or His478. In consequence, modification of Thr285 prevents POPE from approaching the MCR-1 zinc center (**Figure 3C**), leading to a loss of consistency in orientation of bound POPE in the three replicate simulations. Similarly, addition of a second zinc equivalent to the Zn2 site precludes interaction of POPE with the Zn1 site or Thr285. In these simulations, the starting complex involves Zn2 coordination by the "gating" His395 NE2, Glu116 OE1 from the transmembrane domain, and a POPE phosphoryl oxygen atom. Zn2 remains bound for the full 500 ns duration of all three replicate simulations, but makes a variety of interactions as these proceed, most commonly losing contact with His395 and occupying a range of positions coordinated by combinations of POPE phosphoryl oxygens and Glu116. The situation is exacerbated by PEtN addition to Thr285, with Zn2 rapidly dissociating from its crystallographically defined binding site but remaining bound by combinations of the POPE phosphate group, Glu116 and solvent water molecules. Thus, in simulations of di-zinc MCR-1 in both free and PEtN-modified forms of Thr285 POPE

remains bound *via* interactions of the acyl chains with the transmembrane domain, but is neither positioned nor oriented for interaction or reaction with the catalytic Zn1 center (**Figure S5**).

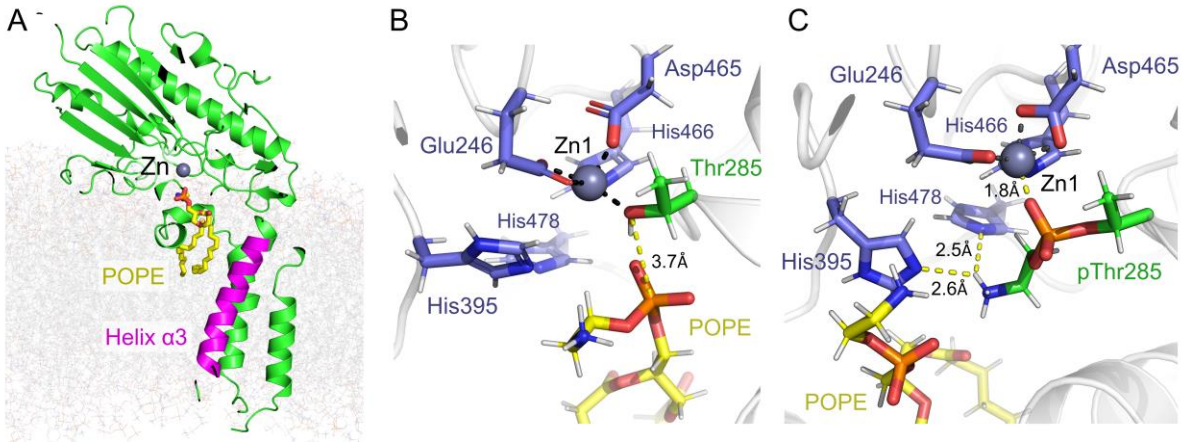

Figure 3. Interactions of POPE with Mono-zinc MCR-1. (A) overall view of POPE (carbon atoms yellow) bound to MCR-1, oriented in the model membrane. Zn ion is shown as gray sphere, MCR-1 transmembrane domain helix α3 (residues 74 - 94) in magenta. (B) Final frame from representative MD simulation of complex of mono-zinc MCR-1 (Thr285 unmodified) with bound POPE. POPE adopts a conformation primed for reaction with Thr285- note proximity of POPE phosphorus atom to Thr285 hydroxyl. (C) Final frame from representative MD simulation of complex of mono-zinc MCR-1 with phosphoethanolamine-modified Thr285 with bound POPE- note interactions of Thr285-bound phosphoethanolamine with "gating" histidine residues His395 and His478. Hydrogen and co-ordination bonds are shown as dashed lines.

Application of Restraints to Zinc Coordination in Simulations of di-Zinc MCR-1

The lability of the Zn2 site is a consistent feature of the simulations described above and, notwithstanding the potential for the additional phosphoryl groups to act as zinc ligands, is not substantially reduced by PEtN addition to Thr285 or by the presence of POPE. However, both the importance to activity of the conserved potential Zn2 ligands Glu116, His395 and His478[15], and our previous molecular simulations suggesting that a second zinc equivalent can facilitate PEtN transfer to the lipid A acceptor[18], indicate a potential role for a candidate Zn2 site. Accordingly, as a further investigation of the architecture and stability of a potential Zn2 site, simulations of di-zinc MCR-1 were repeated with coordinating residues to both Zn1 and Zn2 sites restrained throughout minimization, heating, equilibration and production MD to the crystallographic distances and angles measured in the crystal structure of the catalytic domain in the di-zinc form (PDB 5LRM[15]). In simulations in the absence of POPE, a stable Zn2 site, involving coordination by Glu116 as well as His395 and His478, is observed (**Figure S6A**). On modification by PEtN addition the Thr285-bound phosphoryl group then "bridges" the two zinc ions with each coordinated by an additional oxygen atom (**Figure S6B**). These arrangements were stable and consistent across the two sets of replicate simulations. When POPE is present Zn2 coordination can involve both POPE and Glu116 (**Figure S6C**) but varies between replicates, and is stabilized by PEtN addition to Thr285 to generate an arrangement whereby the Thr285 backbone rotates to enable coordination of Zn2. In consequence the bridging interaction of the two Zn ions by the PEtN phosphoryl group is lost, and Zn2 is coordinated by the phosphoryl groups of both PEtN and POPE (**Figure S6D**). This stable architecture was observed in all three replicate simulations.

Discussion

Despite the increased attention to polymyxin antibiotic resistance that followed the discovery of MCR-1, there remains limited information describing interactions of the complete, full-length, protein, comprising both periplasmic catalytic and inner membrane transmembrane domains, with either its zinc cofactor(s) or its lipidated donor or acceptor substrates. Here we address this knowledge gap by applying extended molecular dynamics (MD) simulations to an homology model of full-length MCR-1 in a membrane environment. In previous MD simulations of the isolated periplasmic catalytic domain[32], based on crystal structures, we established that the overall structure is little affected by phosphorylation of the Thr285 acceptor (which can occur during expression/purification of the recombinant protein and has consequently been observed in experimental structures[15]), or by zinc stoichiometry, but that metal binding to the Zn2 site is unstable. Based on these observations, and on density functional theory (DFT) and *ab initio* calculations on cluster models of the MCR-1 active site[15, 18, 32], we proposed that MCR-1 acts by a "ping-pong" mechanism whereby phosphoethanolamine (PEtN) transfers from a lipidated, phosphatidylethanolamine donor to form a phosphointermediate at Thr285 in a reaction that requires a mono-zinc form of the enzyme. Subsequent PEtN transfer to the lipid A acceptor is then promoted by the di-zinc form of the enzyme, indicating that a second zinc equivalent is recruited to the MCR active site in either the phosphointermediate form or on lipid A binding. Alongside these findings, MD simulations by others, based on the crystal structure of the full-length form of the *N. meningitidis* EptA PEtN transferase, identified this enzyme as able to access an "open" form in which the periplasmic domain repositions relative to the transmembrane domain and "rolls" over the surface of the membrane[14]. We now investigate the dynamic behavior of full-length MCR-1 in extended MD simulations in a model membrane, simulating both mono- and di-zinc forms of the enzyme containing unmodified and phosphoethanolamine-linked forms of Thr285, in the presence and absence of the POPE donor substrate.

At a gross structural level two conclusions are evident. First, the overall structure of the catalytic domain, and the architecture of the MCR-1 active site, appear to be little affected by the presence of the transmembrane domain; as evidenced by comparison with our previous simulations of the periplasmic domain[32], and the consistency of overall RMSD values for simulations carried out under the eight different sets of conditions (**Figure S2**). Second, while there is limited motion of the two domains relative to one another, as adjudged by measurements between the respective centers of mass (**Figure 2**), we do not observe the more profound rearrangements described by Anandan *et al* in their simulations of *N. meningitidis* EptA[14], in which the catalytic domain retains only minimal contact with the transmembrane domain and instead makes extensive interactions with the polar headgroups of the membrane lipids. While under the conditions of our simulations it is possible for the two domains to move relative to one another, in none of the eight combinations of donor substrate, alternative zinc stoichiometry and Thr285 modification did we observe the *c*. 15 Å increase in separation of centers of mass that indicated the profound conformational change described for EptA. This is true in simulations run at both 300 and 310 K, replicating both types of conditions under which this conformational change was observed.

There are several possible explanations for this apparent discrepancy. First, the differing behaviors may indeed reflect mechanistic differences between the two proteins, although their relatively high degree of sequence identity and likely structural conservation may make this unlikely. Second, the choice of parameters, in particular the force field sets, could influence the results of the two sets of simulations. Specifically, the simulations described here were carried out using AMBER (ff14SB force field for protein, lipid17 for lipids, and TIP3P for water), as opposed to GROMACS[34] (GROMOS 54A7[35] for protein, lipid parameters derived from Piggot *et al*[36] (as detailed [14]) and SPC[37] for water) as used

by Anandan *et al*[14]. There are several further differences between the two sets of simulations and their setup- the current work orients the membrane using the PPM server[24] whereas Anandan *et al*. trialed two different depths for their 100% DPPE membrane before finally using a position similar to that obtained with the PPM server. That same orientation was then used for the mixed membrane system (see below).

Third, the current work utilizes a somewhat larger membrane system, extends the duration of the production runs from 100 ns to 500 ns, and employs an 80:20 mix of lipids (POPE:POPG) that differs from the uniform composition (100 % dipalmitoyl-sn-glycero-3-phosphoethanolamine (DPPE)) under which EptA was observed to undergo the striking conformational change described. Notably, such motions were not observed in simulations of EptA that used membranes comprising an 80:20 mixture of 1-palmitoyl-2-palmitoleyl-sn-glycero-3- phosphoethanolamine (PPoPE) and 20% 1,2-dimyristoyl-sn-glycero-3-phospho-(1'-rac)-glycerol (DMPG) i.e. closer to the conditions of those reported here. Anandan *et al* also provide experimental evidence for the existence of an "open" conformation of EptA based on SAXS curves acquired from recombinant protein incorporated into *n*-dodecyl-phosphocholine (DPC) micelles[19], while cautioning that DPC is a known destabilizer of some membrane protein systems. Of note, the "open" conformation was not observed in equivalent experiments using DDM micelles. Overall, while it appears clear that the two domains of bacterial phosphoethanolamine transferases such as EptA or MCR-1 are able to move relative to one another, comparison of available data indicates that in both laboratory investigations and simulations the extent of such movements is strongly dependent upon the local environment.

Our simulations also allowed for investigation of interactions of MCR-1, in both mono- and di-zinc forms and in the presence and absence of PEtN-modified Thr285, with the POPE donor substrate. Notably, in all cases POPE remained associated with MCR-1, due in large part to interactions of the lipid tail with the transmembrane domain. However, close approach of the POPE head group to the active center was possible only in simulations involving the "resting" form of the enzyme, i.e. the mono-zinc form with unmodified Thr285. Under these conditions, POPE, which initially sampled orientations in which the PEtN primary amine contacted the conserved "gating" histidine residues His395 and His478, was (in one of three replicate simulations) able to adopt a stable conformation compatible with subsequent reaction with Thr285, i.e. with the PEtN phosphorous atom approaching Oγ of the Thr285 acceptor. Importantly, this position was not reached in simulations of di-zinc MCR-1, in which the POPE phosphoryl oxygen groups preferentially interacted with the Zn2 ion, or in simulations of the mono-zinc enzyme with Thr285 modified by covalent addition of PEtN, where interaction of the PEtN amine with His395 and/or His478 prevented further entry of POPE into the active site. Taken together with others' experimental observations that the "resting" as-isolated state of the purified recombinant enzyme contains a single zinc equivalent[14, 38], these data then support mechanistic proposals wherein the first stage of the PEtN transfer reaction, i.e. addition of PEtN to Thr285, involves reaction of the donor substrate (e.g. POPE) with the mono-, rather than di-zinc, form of the enzyme.

The existence, and physiological relevance, of a second zinc binding (Zn2) site in MCR enzymes is a matter of continuing uncertainty. In crystal structures of the isolated catalytic domain this site, comprising His395 and His478, is completed by a coordinating Glu, from the second molecule of a crystallographic dimer[15, 39]. In consequence, in simulations of the isolated catalytic domain, in which this interaction is absent, the Zn2 site is unstable[32]. In full-length MCR-1 the conserved residue Glu116, located in the MCR-1 transmembrane domain but positioned close to the catalytic center, is an alternative candidate to complete the Zn2 site. However, under all conditions tested here (presence or absence of POPE and/or PEtN addition to Thr285) the Zn2 site remained unstable unless restraints

were applied to retain coordination by the His395 and His478 side chains. Thus, and consistent with the observations that as-isolated full length EptA and MCR-1 contain a single zinc equivalent, our simulations do not support the existence of a stable di-zinc form of MCR-1 (in the presence/absence of POPE) in either the resting or PEtN-modified (i.e. phosphointermediate) states. Nevertheless, our previous work[18] supports involvement of a second zinc equivalent in PEtN transfer to the lipid A acceptor, implying that the second stage of the reaction involves recruitment of an additional zinc ion. The present data, that do not provide evidence for strong stabilization of the di-zinc form of the enzyme by the PEtN-modified phosphointermediate, then indicate that this recruitment event will likely take place at a later stage in the reaction, potentially during lipid A binding.

Concluding remarks

The data presented here extend our previous computational investigations of MCR-1 by considering, for the first time, the dynamic behavior of the full-length enzyme in a model membrane environment. Over extended (500 ns) simulations of MCR-1 in mono- and di-zinc forms, in both the unmodified "resting" and phosphointermediate forms, the protein is characterized by a relatively limited degree of interdomain flexibility that is consistent across the different states and is little affected by the presence of the POPE donor substrate. In simulations that include bound POPE in the starting structure, POPE remains associated throughout the duration of the trajectories, but the head group samples a range of orientations in the different complexes. In simulations of the "resting" unmodified mono-zinc enzyme bound POPE is however able to access a stable conformation, with its PEtN head group close to the Thr285 acceptor, that we consider represents a plausible ground state complex for the first stage of the PEtN transfer reaction, i.e. phosphointermediate formation. This supports the contention that the mono-zinc form of MCR-1 is able to accept PEtN from a lipidated donor such as POPE and form the phosphointermediate. The relative stability of the Zn1 site in the different complexes contrasts with the instability of the Zn2 site under all conditions trialed, though we caution that the accuracy of such simulations is limited by the well-known challenges of parameterizing transition metal ions such as zinc for molecular dynamics simulations[40], and the metalation state(s) of full-length MCR-1, particularly in the phosphointermediate form, warrant further exploration at higher (quantum mechanical, QM) levels of theory. Extending such investigations to explore the interaction of MCR-1 (and/or related PEtN transferases) with the lipid A acceptor substrate will then represent an important next step in understanding the activity of this increasingly important antimicrobial resistance determinant.

Associated Content

Supporting Information

Equilibration parameters for molecular dynamics simulations of MCR-1 (Table S1); MCR-1 homology model used in simulations (Figure S1); Cα RMSD values for unrestrained MD simulations (Figure S2); comparison of catalytic domain in simulations in isolation and in full-length MCR-1 (Figure S3); active site snapshots from simulations of mono-zinc MCR-1 (Figure S4); active site snapshots from unrestrained simulations of di-zinc MCR-1 with bound POPE (Figure S5); active site snapshots from restrained simulations of di-zinc MCR-1 (Figure S6).

Author Information

Corresponding Authors

James Spencer - School of Cellular and Molecular Medicine, Biomedical Sciences Building, University of Bristol, Bristol, BS8 1TD, United Kingdom; https://orcid.org/0000-0002-4602-0571

E-mail: Jim.Spencer@bristol.ac.uk

Tel: +44-(0)-117-455-8170

Adrian J. Mulholland - Centre for Computational Chemistry, School of Chemistry, University of Bristol, Bristol, BS8 1TS, United Kingdom; https://orcid.org/0000-0003-1015-4567.

E-mail: Adrian.Mulholland@bristol.ac.uk

Tel: +44-(0)-117-456-0524

Authors

Emily Lythell - Centre for Computational Chemistry, School of Chemistry, University of Bristol, Cantock's Close, Bristol BS8 1TS, U.K. and School of Cellular and Molecular Medicine, University of Bristol, University Walk, Bristol BS8 1TD, U.K. https://orcid.org/0000-0003-4513-4275

Reynier Suardiaz - Departamento de Química Física, Facultad de Química, Universidad Complutense, 28040 Madrid, Spain. https://orcid.org/0000-0002-1035-9020

Philip Hinchliffe - School of Cellular and Molecular Medicine, University of Bristol, University Walk, Bristol BS8 1TD, U.K. https://orcid.org/0000-0001-8611-4743

A. Sofia F. Oliveira – Centre for Computational Chemistry, School of Chemistry, University of Bristol, Bristol BS8 1TS, U.K.; https://orcid.org/0000-0001-8753-4950

Marc W. van der Kamp - School of Biochemistry, University of Bristol, University Walk, Bristol BS8 1TD, U.K. https://orcid.org/0000-0002-8060-3359

Author Contributions

Conceptualization- JS, AJM, RS; Methodology- ASFO, RS, EL; Investigation: EL, RS; Writing- original draft preparation- JS; Writing- review and editing: all authors; - Visualization; EL, PH; Supervision- JS, AJM, RS; Funding Acquisition- JS, AJM, RS, MWVdK

Funding Sources

The Royal Society of Chemistry (R19-3409, R20-6912 and R21-6448709305).

MCIN/AEI/10.13039/501100011033 (Grant PID2020-113147GA-I00 and PID2021-122839NB-I00).

The European Research Council under the European Horizon 2020 research and innovation programme (PREDACTED Advanced Grant Agreement no. 101021207).

The U.K. Biotechnology and Biological Sciences Research Council (BB/X009831/1, BB/W003449/1, BB/M026280/1 and BB/M009122/1).

The U.K. Medical Research Council (MR/P007295/1).

The U.K. Engineering and Physical Sciences Research Council (EP/M022609/1, EP/M013219/1),

Oracle for Research.

Notes

The authors declare no competing financial interest.

Data and Software Availability

Supporting data (structures obtained after MD simulations, MD trajectories) are available from the authors on request.

Acknowledgements

This work was carried out using the computational facilities of the Advanced Computing Research Centre, University of Bristol (http://www.bristol.ac.uk/acrc).

We gratefully acknowledge support from the following funders: EL was supported by the Biotechnology and Biological Sciences Research Council-funded South West Biosciences Doctoral Training Partnership [training grant reference BB/M009122/1]. R.S. would like to thank the Royal Society of Chemistry for research funding (Grants R19-3409, R20-6912 and R21-6448709305) and MCIN/AEI/10.13039/501100011033 (Grant PID2020-113147GA-I00 and PID2021-122839NB-I00). PH and JS were supported by the U.K. Medical Research Council (MR/P007295/1). ASFO thanks Oracle for Research for a Fellowship and is a BBSRC Discovery Fellow (grant number BB/X009831/1); she thanks the Biological and Biotechnological Sciences Research Council (BBSRC) for support ([BB/X009831/1] and [BBW003449/1]). MWvdK thanks the Biological and Biotechnological Sciences Research Council (BBSRC) for support (BB/M026280/1). RS, MWvdK, and AJM acknowledge support from the Engineering and Physical Sciences Research Council through the UK Catalysis Hub (EP/M013219/1). AJM and JS acknowledge support from the European Research Council under the European Horizon 2020 research and innovation programme (PREDACTED Advanced Grant Agreement no. 101021207). AJM was supported by the U.K. Engineering and Physical Sciences Research Council (EP/M022609/1).

Abbreviations

AMBER Assisted Model Building with Energy Refinement; AMR antimicrobial resistance; CHARMM Chemistry at Harvard Macromolecular Mechanics; DDM dodecyl-β-d-maltoside; DMPG 1,2-dimyristoyl-sn-glycero-3-phospho-(1'-rac)-glycerol; DPC *n*-dodecyl-phosphocholine; DPPE dipalmitoyl-sn-glycero-3-phosphoethanolamine; LPS lipopolysaccharide; MCR mobile colistin resistance; MD molecular dynamics; PET phosphoethanolaminated threonine; PEtN phosphoethanolamine; POPE palmitoyloleoyl phosphoethanolamine, POPG palmitoyloleoyl

phosphatidylglycerol; PPoPE 1-palmitoyl-2-palmitoleyl-sn-glycero-3- phosphoethanolamine; QM quantum mechanics; RMSD root mean-squared deviation; SAXS small-angle X-ray scattering;

References

(1) Antimicrobial Resistance, C. Global burden of bacterial antimicrobial resistance in 2019: a systematic analysis. *Lancet* **2022**, *399* (10325), 629-655.
(2) O'Neill, J. *Tackling drug-resistant infections globally: Final report and recommendations*; Wellcome Trust, London, U.K., 2016. https://amr-review.org/sites/default/files/160525_Final%20paper_with%20cover.pdf.
(3) Tacconelli, E.; Carrara, E.; Savoldi, A.; Harbarth, S.; Mendelson, M.; Monnet, D. L.; Pulcini, C.; Kahlmeter, G.; Kluytmans, J.; Carmeli, Y.; et al. Discovery, research, and development of new antibiotics: the WHO priority list of antibiotic-resistant bacteria and tuberculosis. *Lancet Infect Dis* **2018**, *18* (3), 318-327.
(4) Soman, R.; Bakthavatchalam, Y. D.; Nadarajan, A.; Dwarakanathan, H. T.; Venkatasubramanian, R.; Veeraraghavan, B. Is it time to move away from polymyxins?: evidence and alternatives. *Eur J Clin Microbiol Infect Dis* **2021**, *40* (3), 461-475.
(5) Falagas, M. E.; Kasiakou, S. K. Toxicity of polymyxins: a systematic review of the evidence from old and recent studies. *Crit Care* **2006**, *10* (1), R27.
(6) Klein, E. Y.; Van Boeckel, T. P.; Martinez, E. M.; Pant, S.; Gandra, S.; Levin, S. A.; Goossens, H.; Laxminarayan, R. Global increase and geographic convergence in antibiotic consumption between 2000 and 2015. *Proc Natl Acad Sci U S A* **2018**, *115* (15), E3463-E3470.
(7) Ledger, E. V. K.; Sabnis, A.; Edwards, A. M. Polymyxin and lipopeptide antibiotics: membrane-targeting drugs of last resort. *Microbiology (Reading)* **2022**, *168* (2). Trimble, M. J.; Mlynarcik, P.; Kolar, M.; Hancock, R. E. Polymyxin: Alternative Mechanisms of Action and Resistance. *Cold Spring Harb Perspect Med* **2016**, *6* (10).
(8) Simpson, B. W.; Trent, M. S. Pushing the envelope: LPS modifications and their consequences. *Nat Rev Microbiol* **2019**, *17* (7), 403-416.
(9) Cox, A. D.; Wright, J. C.; Li, J.; Hood, D. W.; Moxon, E. R.; Richards, J. C. Phosphorylation of the lipid A region of meningococcal lipopolysaccharide: identification of a family of transferases that add phosphoethanolamine to lipopolysaccharide. *J Bacteriol* **2003**, *185* (11), 3270-3277.
(10) Kieffer, N.; Nordmann, P.; Poirel, L. Moraxella Species as Potential Sources of MCR-Like Polymyxin Resistance Determinants. *Antimicrob Agents Chemother* **2017**, *61* (6).
(11) Gerson, S.; Lucassen, K.; Wille, J.; Nodari, C. S.; Stefanik, D.; Nowak, J.; Wille, T.; Betts, J. W.; Roca, I.; Vila, J.; et al. Diversity of amino acid substitutions in PmrCAB associated with colistin resistance in clinical isolates of Acinetobacter baumannii. *Int J Antimicrob Agents* **2020**, *55* (3), 105862. Novovic, K.; Jovcic, B. Colistin Resistance in Acinetobacter baumannii: Molecular Mechanisms and Epidemiology. *Antibiotics (Basel)* **2023**, *12* (3). Potron, A.; Vuillemenot, J. B.; Puja, H.; Triponney, P.; Bour, M.; Valot, B.; Amara, M.; Cavalie, L.; Bernard, C.; Parmeland, L.; et al. ISAba1-dependent overexpression of eptA in clinical strains of Acinetobacter baumannii resistant to colistin. *J Antimicrob Chemother* **2019**, *74* (9), 2544-2550.
(12) Liu, Y. Y.; Wang, Y.; Walsh, T. R.; Yi, L. X.; Zhang, R.; Spencer, J.; Doi, Y.; Tian, G.; Dong, B.; Huang, X.; et al. Emergence of plasmid-mediated colistin resistance mechanism MCR-1 in animals and human beings in China: a microbiological and molecular biological study. *Lancet Infect Dis* **2016**, *16* (2), 161-168.
(13) Ling, Z.; Yin, W.; Shen, Z.; Wang, Y.; Shen, J.; Walsh, T. R. Epidemiology of mobile colistin resistance genes mcr-1 to mcr-9. *J Antimicrob Chemother* **2020**, *75* (11), 3087-3095.
(14) Anandan, A.; Evans, G. L.; Condic-Jurkic, K.; O'Mara, M. L.; John, C. M.; Phillips, N. J.; Jarvis, G. A.; Wills, S. S.; Stubbs, K. A.; Moraes, I.; et al. Structure of a lipid A phosphoethanolamine transferase suggests how conformational changes govern substrate binding. *Proc Natl Acad Sci U S A* **2017**, *114* (9), 2218-2223.
(15) Hinchliffe, P.; Yang, Q. E.; Portal, E.; Young, T.; Li, H.; Tooke, C. L.; Carvalho, M. J.; Paterson, N. G.; Brem, J.; Niumsup, P. R.; et al. Insights into the Mechanistic Basis of Plasmid-Mediated Colistin Resistance from Crystal Structures of the Catalytic Domain of MCR-1. *Sci Rep* **2017**, *7*, 39392.

(16) Stojanoski, V.; Sankaran, B.; Prasad, B. V.; Poirel, L.; Nordmann, P.; Palzkill, T. Structure of the catalytic domain of the colistin resistance enzyme MCR-1. *BMC Biol* **2016**, *14* (1), 81.
(17) Wanty, C.; Anandan, A.; Piek, S.; Walshe, J.; Ganguly, J.; Carlson, R. W.; Stubbs, K. A.; Kahler, C. M.; Vrielink, A. The structure of the neisserial lipooligosaccharide phosphoethanolamine transferase A (LptA) required for resistance to polymyxin. *J Mol Biol* **2013**, *425* (18), 3389-3402.
(18) Suardiaz, R.; Lythell, E.; Hinchliffe, P.; van der Kamp, M.; Spencer, J.; Fey, N.; Mulholland, A. J. Catalytic mechanism of the colistin resistance protein MCR-1. *Org Biomol Chem* **2021**, *19* (17), 3813-3819.
(19) Anandan, A.; Dunstan, N. W.; Ryan, T. M.; Mertens, H. D. T.; Lim, K. Y. L.; Evans, G. L.; Kahler, C. M.; Vrielink, A. Conformational flexibility of EptA driven by an interdomain helix provides insights for enzyme-substrate recognition. *IUCrJ* **2021**, *8* (Pt 5), 732-746.
(20) Sali, A.; Blundell, T. L. Comparative protein modelling by satisfaction of spatial restraints. *J Mol Biol* **1993**, *234* (3), 779-815.
(21) Schrodinger, LLC. The PyMOL Molecular Graphics System, Version 1.8. 2015.
(22) Bayly, C. I.; Cieplak, P.; Cornell, W.; Kollman, P. A. A well-behaved electrostatic potential based method using charge restraints for deriving atomic charges: the RESP model. *The Journal of Physical Chemistry* **1993**, *97* (40), 10269-10280. Dupradeau, F.-Y.; Pigache, A.; Zaffran, T.; Savineau, C.; Lelong, R.; Grivel, N.; Lelong, D.; Rosanski, W.; Cieplak, P. The R.E.D. tools: advances in RESP and ESP charge derivation and force field library building. *Physical Chemistry Chemical Physics* **2010**, *12* (28), 7821-7839, 10.1039/C0CP00111B. *Gaussian 16 Rev. C.01*; Wallingford, CT, 2016. (accessed. Vanquelef, E.; Simon, S.; Marquant, G.; Garcia, E.; Klimerak, G.; Delepine, J. C.; Cieplak, P.; Dupradeau, F. Y. R.E.D. Server: a web service for deriving RESP and ESP charges and building force field libraries for new molecules and molecular fragments. *Nucleic Acids Res* **2011**, *39* (Web Server issue), W511-517. Wang, F.; Becker, J.-P.; Cieplak, P.; Dupradeau, F.-Y. RED Python: Object oriented programming for Amber force fields. In *Abstracts of Papers of the American Chemical Society*, 2014; AMER CHEMICAL SOC 1155 16TH ST, NW, WASHINGTON, DC 20036 USA: Vol. 247.
(23) Brooks, B. R.; Brooks, C. L., 3rd; Mackerell, A. D., Jr.; Nilsson, L.; Petrella, R. J.; Roux, B.; Won, Y.; Archontis, G.; Bartels, C.; Boresch, S.; et al. CHARMM: the biomolecular simulation program. *J Comput Chem* **2009**, *30* (10), 1545-1614. Jo, S.; Kim, T.; Iyer, V. G.; Im, W. CHARMM-GUI: a web-based graphical user interface for CHARMM. *J Comput Chem* **2008**, *29* (11), 1859-1865.
(24) Lomize, M. A.; Pogozheva, I. D.; Joo, H.; Mosberg, H. I.; Lomize, A. L. OPM database and PPM web server: resources for positioning of proteins in membranes. *Nucleic Acids Res* **2012**, *40* (Database issue), D370-376.
(25) Wu, E. L.; Cheng, X.; Jo, S.; Rui, H.; Song, K. C.; Davila-Contreras, E. M.; Qi, Y.; Lee, J.; Monje-Galvan, V.; Venable, R. M.; et al. CHARMM-GUI Membrane Builder toward realistic biological membrane simulations. *J Comput Chem* **2014**, *35* (27), 1997-2004.
(26) Maier, J. A.; Martinez, C.; Kasavajhala, K.; Wickstrom, L.; Hauser, K. E.; Simmerling, C. ff14SB: Improving the Accuracy of Protein Side Chain and Backbone Parameters from ff99SB. *J Chem Theory Comput* **2015**, *11* (8), 3696-3713.
(27) Gould, I.; Skjevik, A.; Dickson, C.; Madej, B.; Walker, R. Lipid17: A comprehensive AMBER force field for the simulation of zwitterionic and anionic lipids. *Manuscript in preparation* **2018**.
(28) Lee, J.; Cheng, X.; Swails, J. M.; Yeom, M. S.; Eastman, P. K.; Lemkul, J. A.; Wei, S.; Buckner, J.; Jeong, J. C.; Qi, Y.; et al. CHARMM-GUI Input Generator for NAMD, GROMACS, AMBER, OpenMM, and CHARMM/OpenMM Simulations Using the CHARMM36 Additive Force Field. *J Chem Theory Comput* **2016**, *12* (1), 405-413. Lee, J.; Hitzenberger, M.; Rieger, M.; Kern, N. R.; Zacharias, M.; Im, W. CHARMM-GUI supports the Amber force fields. *J Chem Phys* **2020**, *153* (3), 035103.
(29) Jo, S.; Kim, T.; Im, W. Automated builder and database of protein/membrane complexes for molecular dynamics simulations. *PLoS One* **2007**, *2* (9), e880. Jo, S.; Lim, J. B.; Klauda, J. B.; Im, W. CHARMM-GUI Membrane Builder for mixed bilayers and its application to yeast membranes. *Biophys J* **2009**, *97* (1), 50-58. Lee, J.; Patel, D. S.; Stahle, J.; Park, S. J.; Kern, N. R.; Kim, S.; Lee, J.; Cheng, X.;

Valvano, M. A.; Holst, O.; et al. CHARMM-GUI Membrane Builder for Complex Biological Membrane Simulations with Glycolipids and Lipoglycans. *J Chem Theory Comput* **2019**, *15* (1), 775-786.
(30) Peters, M. B.; Yang, Y.; Wang, B.; Fusti-Molnar, L.; Weaver, M. N.; Merz, K. M., Jr. Structural Survey of Zinc Containing Proteins and the Development of the Zinc AMBER Force Field (ZAFF). *J Chem Theory Comput* **2010**, *6* (9), 2935-2947.
(31) Miyamoto, S.; Kollman, P. A. Settle: An analytical version of the SHAKE and RATTLE algorithm for rigid water models. *Journal of Computational Chemistry* **1992**, *13* (8), 952-962.
(32) Lythell, E.; Suardiaz, R.; Hinchliffe, P.; Hanpaibool, C.; Visitsatthawong, S.; Oliveira, A. S. F.; Lang, E. J. M.; Surawatanawong, P.; Lee, V. S.; Rungrotmongkol, T.; et al. Resistance to the "last resort" antibiotic colistin: a single-zinc mechanism for phosphointermediate formation in MCR enzymes. *Chem Commun (Camb)* **2020**, *56* (50), 6874-6877.
(33) Hu, M.; Guo, J.; Cheng, Q.; Yang, Z.; Chan, E. W. C.; Chen, S.; Hao, Q. Crystal Structure of Escherichia coli originated MCR-1, a phosphoethanolamine transferase for Colistin Resistance. *Sci Rep* **2016**, *6*, 38793. Ma, G.; Zhu, Y.; Yu, Z.; Ahmad, A.; Zhang, H. High resolution crystal structure of the catalytic domain of MCR-1. *Sci Rep* **2016**, *6*, 39540. Wei, P.; Song, G.; Shi, M.; Zhou, Y.; Liu, Y.; Lei, J.; Chen, P.; Yin, L. Substrate analog interaction with MCR-1 offers insight into the rising threat of the plasmid-mediated transferable colistin resistance. *FASEB J* **2018**, *32* (2), 1085-1098.
(34) Van Der Spoel, D.; Lindahl, E.; Hess, B.; Groenhof, G.; Mark, A. E.; Berendsen, H. J. GROMACS: fast, flexible, and free. *J Comput Chem* **2005**, *26* (16), 1701-1718.
(35) Schmid, N.; Eichenberger, A. P.; Choutko, A.; Riniker, S.; Winger, M.; Mark, A. E.; van Gunsteren, W. F. Definition and testing of the GROMOS force-field versions 54A7 and 54B7. *Eur Biophys J* **2011**, *40* (7), 843-856.
(36) Piggot, T. J.; Holdbrook, D. A.; Khalid, S. Electroporation of the E. coli and S. Aureus membranes: molecular dynamics simulations of complex bacterial membranes. *J Phys Chem B* **2011**, *115* (45), 13381-13388.
(37) Berendsen, H.; Postma, J.; Van Gunsteren, W.; Hermans, a. J.; Pullman, B. Interaction Models for Water in Relation to Protein Hydration. In *Intermolecular Forces*, Pullman, B. Ed.; Reidel, 1981; pp 331-342.
(38) Xu, Y.; Wei, W.; Lei, S.; Lin, J.; Srinivas, S.; Feng, Y. An Evolutionarily Conserved Mechanism for Intrinsic and Transferable Polymyxin Resistance. *mBio* **2018**, *9* (2).
(39) Coates, K.; Walsh, T. R.; Spencer, J.; Hinchliffe, P. 1.12 A resolution crystal structure of the catalytic domain of the plasmid-mediated colistin resistance determinant MCR-2. *Acta Crystallogr F Struct Biol Commun* **2017**, *73* (Pt 8), 443-449.
(40) Li, P.; Merz, K. M., Jr. Metal Ion Modeling Using Classical Mechanics. *Chem Rev* **2017**, *117* (3), 1564-1686.